MAUSAM, **77**, 3 (July 2026),1019-1034

MAUSAM

DOI: https://doi.org/10.54302/mausam.v77i3.6819
Homepage: https://mausamjournal.imd.gov.in/index.php/MAUSAM

UDC No.551.524:502.131.1:551.583.7

Assessing the impact of land use change in the Simulation of extreme temperature events over Odisha during May 2015

S. K. SAHOO[1,2], K. C. GOUDA [2,3,*], S. HIMESH[2] and RAJESH KUMAR SAHU[2]

[1]*National Centre for Medium-Range Weather Forecasting, Ministry of Earth Sciences, Noida, Uttar Pradesh, India*

[2]*CSIR Fourth Paradigm Institute, Wind Tunnel Road, Bangalore-37, India*

[3]*Academy of Scientific and Innovative Research (AcSIR), Ghaziabad, UP, India*

(*Received 28 August 2024, Accepted 7 March 2026*)

***Corresponding author's email: kcgouda.4pi@csir.res.in**

सार – मई 2015 के तीसरे और चौथे सप्ताह में ओडिशा में लगभग दो सप्ताह तक चलने वाली एक अभूतपूर्व ग्रीष्म लहर (Heat wave) आई, जिसके परिणामस्वरूप मौसम संबंधी खतरे उत्पन्न हुए। इस अध्ययन में, 25-27 मई 2015 को अत्यधिक तापमान की एक घटना (Extreme Temperature Event - ETE) घटित हुई, क्योंकि ओडिशा राज्य के लगभग 15 मौसम अवलोकन केंद्रों में अधिकतम तापमान 45°C से अधिक दर्ज किया गया, जिसके परिणामस्वरूप तीव्र ग्रीष्म लहर चली। इस अध्ययन में विभिन्न भूमि उपयोग परिदृश्यों (Land use scenarios) का उपयोग करके क्षेत्रीय स्तर पर ऐसी ETE का अनुकरण करने के लिए मेसोस्केल मॉडलिंग फ्रेमवर्क (WRF4.0) को कॉन्फ़िगर और अनुकूलित किया गया है। भारतीय अंतरिक्ष अनुसंधान संगठन (ISRO) के डेटा से वर्तमान भूमि उपयोग परिदृश्य के आधार पर समय-समूह अनुकरण (Time-ensemble simulation) पर पाया गया अधिकतम तापमान, भारत मौसम विज्ञान विभाग (IMD) के मौसम केंद्रों की तुलना में अमेरिकी भूवैज्ञानिक सर्वेक्षण (USGS) के डेटा-आधारित अनुकरणों से अधिक सटीक है। IMD स्टेशन-स्तरीय अवलोकनों के संदर्भ में ओडिशा में अनुक्रमित अधिकतम तापमान की औसत प्रतिशत त्रुटि 25 मई 2015 को क्रमशः 1.6% (ISRO) और 3% (USGS) थी, जबकि 26 मई 2015 को क्रमशः 4.2% (ISRO) और 4.7% (USGS) थी। ISRO डेटा (अधिक शहरीकृत) पर आधारित अनुकरण की तुलना में, ओडिशा में विभिन्न स्थानों पर अनुक्रमित क्षैतिज सतही हवा USGS डेटा पर आधारित अनुकरण के लिए अपेक्षाकृत अधिक है। भूमि उपयोग में परिवर्तनों का तात्पर्य सतही खुरदरेपन की लंबाई (Surface roughness length) में वृद्धि से है, जिसके परिणामस्वरूप सतही हवा की गति में कमी आती है। मॉडल से आर्द्रता, बहिर्गामी दीर्घतरंग विकिरण (Outgoing Longwave Radiation - OLR), संवहनी उपलब्ध स्थितिज ऊर्जा (Convective Available Potential Energy - CAPE) और संवहनी अवरोध (Convective Inhibition - CIN) आदि का विश्लेषण करके इसके गतिक पहलुओं का भी अन्वेषण किया गया है। पुनः विश्लेषण उत्पादों (Reanalysis products) के साथ इसका सत्यापन मॉडल के उस प्रदर्शन का समर्थन करता है जो क्षेत्रीय ग्रीष्म लहर के अनुकूल वातावरण को दर्ज करता है। भूमि उपयोग विश्लेषण से पता चलता है कि 1992 और 2015 के बीच राज्य-व्यापी शहरीकरण में लगभग 0.4% की वृद्धि हुई थी, जिसमें सबसे अधिक प्रतिशत वृद्धि भुवनेश्वर, संबलपुर, झारसुगुडा और सुंदरगढ़ जिले के राउरकेला जैसे शहरों में हुई, जहाँ नियमित रूप से मई के महीने में ग्रीष्म लहर का अनुभव होता है और इसे अनुकूलित एवं कैलिब्रेटेड मॉडल कॉन्फ़िगरेशन द्वारा सटीक रूप से अनुक्रमित किया गया है। शहरी विस्तार और बदलती फसल प्रणालियों के संदर्भ में भूमि-उपयोग परिवर्तन, मानवजनित गतिविधियों में वृद्धि के साथ, अधिकतम तापमान में वृद्धि से सीधे तौर पर जुड़े हुए हैं।

ABSTRACT. An unprecedented heat wave lasting approximately two weeks occurred in Odisha during the third and fourth weeks of May 2015, resulting in meteorological hazards. In this study, an extreme temperature event (ETE) occurred on 25-27th May 2015, with about 15 meteorological observation stations in the state of Odisha recording maximum temperatures exceeding 45 °C, resulting in an intense heat wave. The mesoscale modeling framework (WRF4.0) is configured and optimized to simulate ETE at the regional scale in this study using different land-use scenarios. The maximum temperature from a time-ensemble simulation using the current land-use scenario based on Indian Space Research Organization (ISRO) data is found to be more accurate than simulations based on US Geological Survey (USGS)

data at India Meteorological Department (IMD) meteorological stations. The mean percentage errors of simulated maximum temperatures over Odisha with respect to IMD station-scale observations are 1.6% (ISRO) and 3% (USGS) on 25th May 2015, and 4.2% (ISRO) and 4.7% (USGS) on 26th May 2015, respectively. Compared with the simulation based on ISRO data (more urbanized), the simulated horizontal surface wind at the different locations in Odisha is generally higher in the simulation based on USGS data. Changes in land use increase the roughness length, reducing surface wind speed. The dynamical aspects are also explored by analyzing humidity, outgoing longwave radiation (OLR), Convective Available Potential Energy (CAPE), and Convective Inhibition (CIN), etc., from the model and validated with the reanalysis products, which support the model performance in capturing the conducive environment resulting in a regional heat wave. The land use analysis reveals that the state-wide increase in urbanization between 1992 and 2015 was about 0.4%, with the highest percentage increase occurring in cities like Bhubaneswar, Sambalpur, Jharsuguda, and Rourkela in the Sundergarh district, which regularly experience the heat wave in the month of May, and the same are accurately simulated by the optimized and calibrated model configuration. Land-use change, including urban expansion and shifting cropping patterns, along with increased anthropogenic activities, is directly linked to the rise in maximum temperatures.

Keywords – Heat-wave, Extreme temperature, WRF Model, ISRO, USGS, Urbanization.

1. Introduction

One of the most important natural resources on Earth is the landmass. Both human survival and the essential environmental processes depend on it. Land use is crucial to achieving long-term economic development and social benefits. Human demand for land use has increased over time. As a result, urbanization, reduced agricultural land, deforestation, and other anthropogenic activities significantly alter the Earth's landscape, posing several challenges (Intergovernmental Panel on Climate Change, IPCC 2007). India experienced an increasing trend in the frequency and duration of severe heat waves between 1991 and 2000 (Pai *et al*., 2004 and 2013), resulting in significant loss of life (De and Sinha Ray, 2000). In 1998, 650 people died in Odisha due to an intense heat wave (De and Mukhopadhyay, 1998). Around the globe, there has been a significant amount of research done on the situation and processes behind large-scale extreme temperature events, particularly in North America (Gershunov *et al.,* 2009; Lau & Nath, 2012) and Europe (Fink *et al.,* 2004; Black *et al.,* 2004; Schar *et al*., 2004; Dasari *et al.,* 2014). The urbanization and land use land cover (LULC) change patterns (Goswami *et al.,* 2010; Gogoi *et al*., 2019) drastically increase the daily maximum temperature (ground temperature) and the Diurnal Temperature Range (DTR) in urban cities, affecting the frequency and intensity of hot days as well as rainfall. Changes in land use and urbanization modulate the incidence of heat waves (Mohan and Kandya, 2015; Halder *et al*., 2016; Swain *et al*., 2017). In addition, LULC and urbanization have been linked to atmospheric aerosol emissions (Pandey *et al*., 2017; Kumar *et al*., 2017), which generally modify surface temperatures. Using observational datasets, previous studies (Hulme *et al*., 1994; Li *et al*., 2004; Chung *et al*., 2004; Ren *et al*., 2008; Fujibe, 2008) have documented climate change and its contribution to increased surface temperatures driven by urbanization. Understanding the occurrence of heat waves in a particular geographic region can be enhanced by analyzing long-term temperature (daily maximum) trends (Li *et al*., 2015; Devi *et al*., 2023).

Thermodynamic conditions in the pre-monsoon season are often summarized using indices such as Convective Available Potential Energy (CAPE) and Convective Inhibition (CIN), which provide compact diagnostics of instability, moisture availability, and the "cap" that limits convective initiation; these diagnostics are particularly relevant in heat-wave environments where suppressed convection can allow extreme surface heating to persist (Mbokodo *et al.,* 2020; You and Wang, 2021; Sahu *et al.,* 2022). Over eastern India (including Odisha), climatological analyses for 1987–2016 show coherent pre-monsoon patterns in CAPE and CIN, with relatively higher CAPE and lower CIN over coastal Odisha and West Bengal (Sahu *et al.,* 2022; Tyagi *et al*., 2022; Mahato and Satyanarayan, 2025). Long-term station analyses over Bhubaneswar, Kolkata, and Ranchi show increasing humidity and indicate that thermodynamic-index thresholds can shift across decades, requiring region- and period-specific interpretation under climate change (Sahu *et al.,* 2020; Sethi *et al*., 2025; Beuria *et al*., 2025).

Only a few studies are available on the resulting changes in surface temperature from LULC changes. Those studies are limited to select metropolitan cities (Nayak and Mandal, 2012; Jalan and Sharma, 2014; Grover and Singh, 2015; Singh *et al.,* 2017) and focus primarily on urbanization (Ren *et al*., 2008; Jiang *et al*., 2015; Fan *et al*., 2017). The combined effects of LULC changes and greenhouse gases, of which about 50% was attributed to land-use change, are causing surface temperatures across western India to rise by about 0.13 °C/decade (Nayak and Mandal, 2012). Additionally, the 53% rise in the built-up area was attributed to an area covering 26.4% (2001) and 65.3% (2011) of New Delhi with DTR below 11°C (Mohan *et al*., 2011 and 2012; Mohan and Kandya, 2015). The impact of land use change on climate variability in Indian regions has been the subject of a limited number of scientific studies (Niyogi *et al*., 2011; Mohan and Kandya, 2015; Nayak and Mandal, 2012 and 2019), and the overall picture of this impact on the coastal state of Odisha remains unclear. There are limited studies on heat waves (Gouda *et al*., 2017) linked to changes in LULC

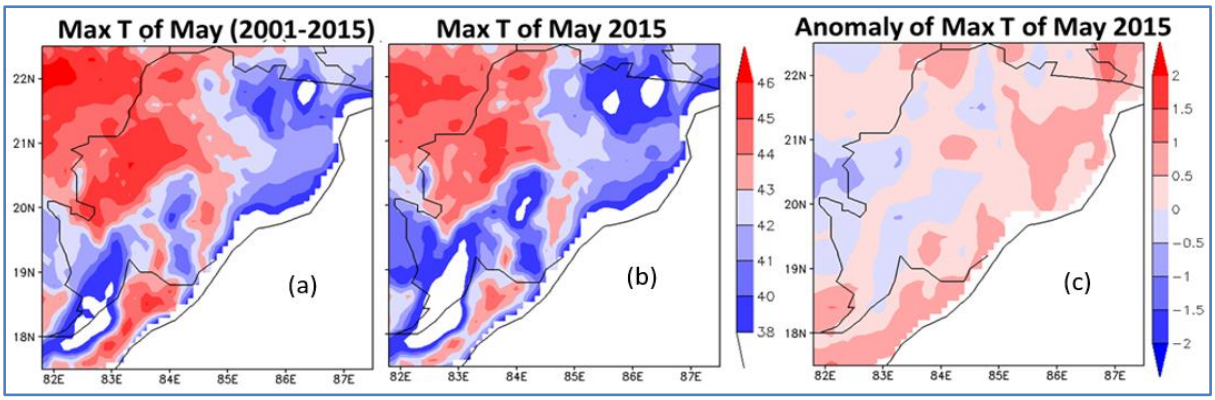

Figs. 1(a-c). The spatial distribution of monthly maximum temperature (May) attained by the meteorological stations from 2001 to 2015 (left panel), for May 2015 (middle), and the anomaly of maximum temperature for the year 2015 (right panel)

(Gogoi *et al*., 2019) and urbanization in Odisha, which has been witnessing massive mining over the past few decades. Furthermore, limited studies have examined the link between land-use change and heat waves in the state of Odisha, one of India's most vulnerable regions to natural disasters.

This study uses multiple observations from different sources of maximum temperature to examine variations across the state of Odisha and their relationship with land-use change, along with simulations based on various land uses (over the heat wave period) with different reference years covering 1992 to 2015. Accordingly, evaluating thermodynamic indices alongside maximum temperatures helps interpret how LULC changes modulate moisture, stability, and convective inhibition during the May 2015 heat wave (Rao *et al*., 2021; Sahu *et al*., 2022; Sahu *et al*., 2024).

2. Data and methodology

2.1. *Event description*

During the third and fourth weeks of May 2015, the state of Odisha had an unprecedented heat wave that lasted for around two weeks. The intriguing aspect of the episodic heat wave is that it mainly affected the state of Odisha and persisted throughout the late pre-monsoon season. During the intense heat wave, the highest daily temperature in about 15 cities exceeded 45 °C, and May 25–27, 2015, was designated as a red zone by the India Meteorological Department (IMD). This prompted us to study the extreme temperature event (heat wave) over Odisha from 24th May to 27th May 2015.

2.2. *Observational analysis*

For long-term trend analysis over the state of Odisha, the high-resolution (0.25 ° × 0.25 °) gridded temperature data from IMD was used for the period 1969–2015, and the high-resolution (~9 km) ERA5 land was used for the period 2001-2015. The spatial distribution of the monthly maximum temperature attained by each grid for 15 years is presented in Fig. 1 (left panel). This figure shows that Odisha's western and central regions experienced temperatures above 43 °C over the last 15 years. The coastal districts of Odisha experienced temperatures of about 38-41 °C during that period. For May 2015 (Fig. 1 (middle panel), most of the western part of Odisha experienced more than 43 °C, along with the central part. According to IMD, more than 12 meteorological stations recorded a maximum temperature of 45 or higher for three consecutive days (25-27 May 2015) during the last week of May 2015, as shown in this figure. The anomaly (Fig. 1; right panel) in maximum temperature relative to the long-term mean shows that it increased over coastal and central Odisha, whereas it decreased over southern Odisha. This massive change in maximum temperature across the coastal districts is due to changes in LULC patterns, as suggested by Gogoi *et al.* (2019), and also to our land-use analysis plot discussed in a later section.

Based on IMD observations, the daily maximum temperature (station scale) of May for the years 1969–2015 is examined and presented in Fig. 2a. The 47-year (1969-2015) analysis reveals that the average maximum temperature over the state is 45 ℃, with a standard deviation (variability) of roughly 1.8 ℃ across years. In 1998, Titilagarh in western Odisha recorded the highest temperature to date at 50 °C. The maximum temperature trend for the study period (1969–2015) likewise shows a positive value (0.04 ℃/year), suggesting that increases in LULC and urbanization are causing summer (May) temperatures in Odisha to rise. A decadal trend in the maximum temperature recorded each day across all of Odisha is calculated, and the trend is shown in Fig. 2b. The 1989–1998 decade showed a substantial

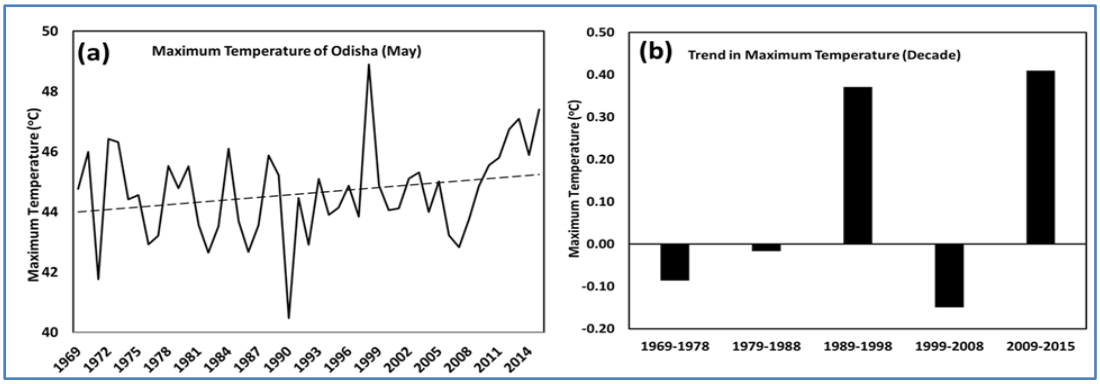

Figs. 2(a&b). (a) Interannual Variability in the Maximum Temperature attained at a station over Odisha from 1969-2015 (b) Trend in the Maximum Temperature over Odisha during the last five decades computed from IMD Observations

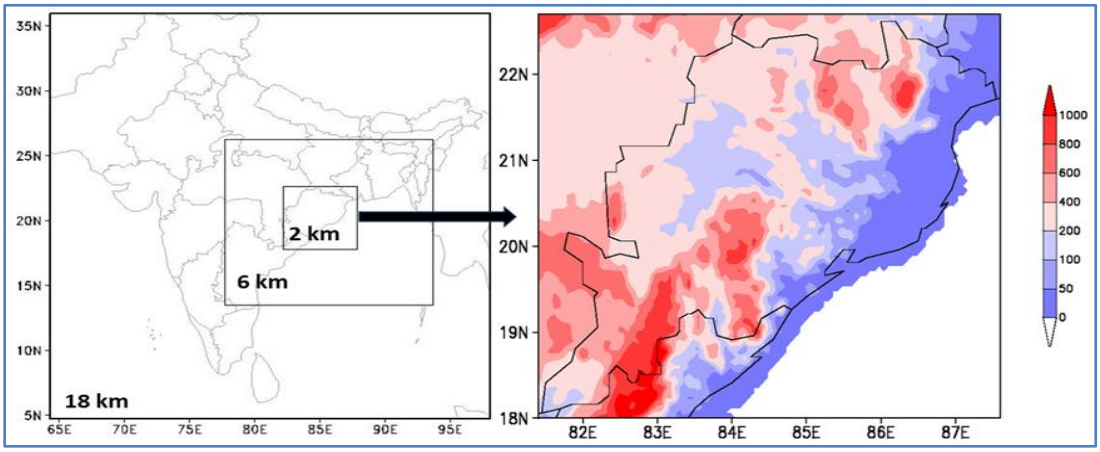

Fig. 3 Spatial plot of the Model domain with Terrain height (m) for the Extreme Temperature simulation

positive trend (0. 37 ℃/year) in trend analysis, which was followed by a negative trend (-0.15 ℃/year). The maximum temperature trend has been rising by 0.41 ℃ per year over Odisha during the most recent period (2009–2015). These variations in maximum temperature are due to the possible impact of land use change over a period of time, as supported by earlier studies (Gogoi *et al*., 2019).

2.3. *Simulated event analysis*

The primary objective of this section was to evaluate the model's ability to replicate significant weather phenomena, such as heat waves driven by extremely high temperatures across a particular area, using two sets of land-use data from different sources with different reference dates. Such events must be predicted well in advance, which calls for a model with known accuracy and forecast skill.

2.4. *Methodology*

The WRF (Version 4.0) model, a well-known numerical weather prediction system, was employed in atmospheric research and forecasting (Skamarock *et al*., 2019). The WRF model is highly customizable and offers options for cloud microphysics, convection, radiation, and planetary boundary layer (PBL) physics. The selection of appropriate physics schemes is essential for dependable surface temperature prediction (Mooney *et al*., 2013; García-Díez *et al*., 2015; Varga and Breuer, 2020).

A configuration with three nested domains having horizontal resolutions of 36, 12 & 2 km, respectively, was used in this study (Fig. 3). The WRF model physics options included the WSM6 microphysics (Hong and Lim, 2006) scheme, the Grell-Devenyi ensemble scheme (Grell and Devenyi, 2002) for cumulus, the Yonsei University (YSU) scheme (Hong *et al*., 2006) for PBL, and the rapid radiative transfer model (RRTM) long wave (Mlawer *et al*., 1997) and Dudhia short wave (Dudhia, 1989). Through feedback between the outer & inner domains, a three-nested domain configuration was implemented to dynamically downscale the original state and reflect the impact of large-scale circulation on urban extreme events. The model configuration consists of 40 vertical levels, with higher levels in the lower troposphere, and a top level at 50 hPa.

TABLE 1

Model Configuration for Extreme Temperature (Heat Wave) Simulation

Dynamics	Non-hydrostatic
Number of domains	Three nested domains
Horizontal resolutions	18 km (outermost domain), 6 km (inner domain), and 2 km (innermost domain).
Number of grid points	*X-direction* 183, 259, and 277, *Y-direction 183, 220, and 250 points for Outermost, inner, and innermost domains*, respectively.
Map projection	Mercator
Horizontal grid	Arakawa C-grid
Vertical coordinate	Terrain following hydrostatic with 40 sigma levels
Time integration	Third-order Runge–Kutta
Spatial difference scheme	Sixth-order centered difference
Microphysics	WSM6 scheme
Radiation	LW: RRTM SW: Dudhia
Cumulus parameterization	Grell-Devenyi ensemble scheme (only for the outer domain)
PBL parameterization	YSU scheme
Land surface parameterization	Thermal diffusion

The WRF model simulation uses the United States (US) National Centers for Environmental Prediction (NCEP) FNL (Final) operational data at (1^{o}x1^{o}) resolution for the initial and lateral boundary conditions. The Global Data Assimilation System (GDAS) prepares these data operationally every six hours, continuously collecting observational data from the Global Telecommunications System (GTS). The model land surface parameters, such as terrain height, land use (USGS and ISRO-24 categories), and vegetation fraction, were extracted from the US Geological Survey data sets.

For this study, two simulation experiments were carried out: a control simulation using land-use data from the USGS with the reference year 1992-93 (Loveland *et al*., 2000) based on the less urbanized scenario (old data) and a test simulation using data from the ISRO (Gharai *et al*., 2018) with the reference year 2015-16 based on the up-to-date land use data representing more urban scenario. Time-ensemble simulations (3 initial conditions) from 00UTC, 06UTC, and 12UTC on May 24, 2015, to 00UTC on May 27, 2015, provide the framework for the analysis and diagnostics. This study uses a time-ensemble simulation approach to improve WRF model performance in handling system uncertainties. The model configuration details for the extreme event simulation are presented in Table 1. In parallel, process-based studies using WRF experiments show that thermodynamic indices are sensitive to topography; for instance, modifying Chhota Nagpur Plateau topography alters CTI, HI, CIN, and SWEAT and produces spatial impacts extending into parts of Odisha (Sahu *et al.*, 2023; Sahu *et al.*, 2024)

3. Results and Discussion

3.1. *Analysis of land use and land cover*

Over the past 20 years, the built-up area of Odisha has increased by 0.4%. Cities such as Bhubaneswar, Sambalpur, Jharsuguda, and Rourkela in the Sundergarh district, and the coastal districts that experienced the extreme May temperatures, have seen the greatest rise in urbanization (Fig. 4). The most recent land-use data also show the emergence of numerous new, dispersed urban built-up patches throughout the state. As evidenced by the land-use analysis figure, there was a drop in croplands and dense vegetation, and an increase of almost 83% in the urban area surrounding Bhubaneswar (Swain *et al*., 2017) between 2000 and 2015. So, urban expansion and LULC changes over time resulted in a net decrease in vegetation due to anthropogenic activities, affecting local weather systems and enhancing heat waves.

3.2. *Large-scale circulation*

The averaged wind circulation patterns from the ERA5 reanalysis and model simulation at the lower (i.e., 850 hPa) and upper (i.e., 200 hPa) troposphere levels throughout the week of extreme temperatures that resulted in a heat wave are presented in Fig. 5a and 5b. This simulation shows how extreme temperatures cause heat waves, linked to large-scale atmospheric anomalies that connect quasi-stationary Rossby waves over mid latitudes, clear skies, reduced soil moisture, and persistent subtropical highs. (Ratnam *et al*. 2016). The simulation also agrees well with the observed circulation pattern described in earlier studies (Rohini *et al*., 2016; Ratnam *et al*., 2016).

3.3. *Analysis of surface wind*

The model simulated horizontal surface wind at different locations across the state, as shown in Fig. 6. All locations exhibit lower surface wind in more urbanized scenarios than in less urbanized ones. This is to be expected, as a change in land use increases the surface roughness length, reducing surface wind speed due to the additional drag from the impervious surface.

3.4. *Analysis of maximum temperature*

During the study period, Odisha state witnessed severe extreme temperatures for almost 1 - 2 weeks. The

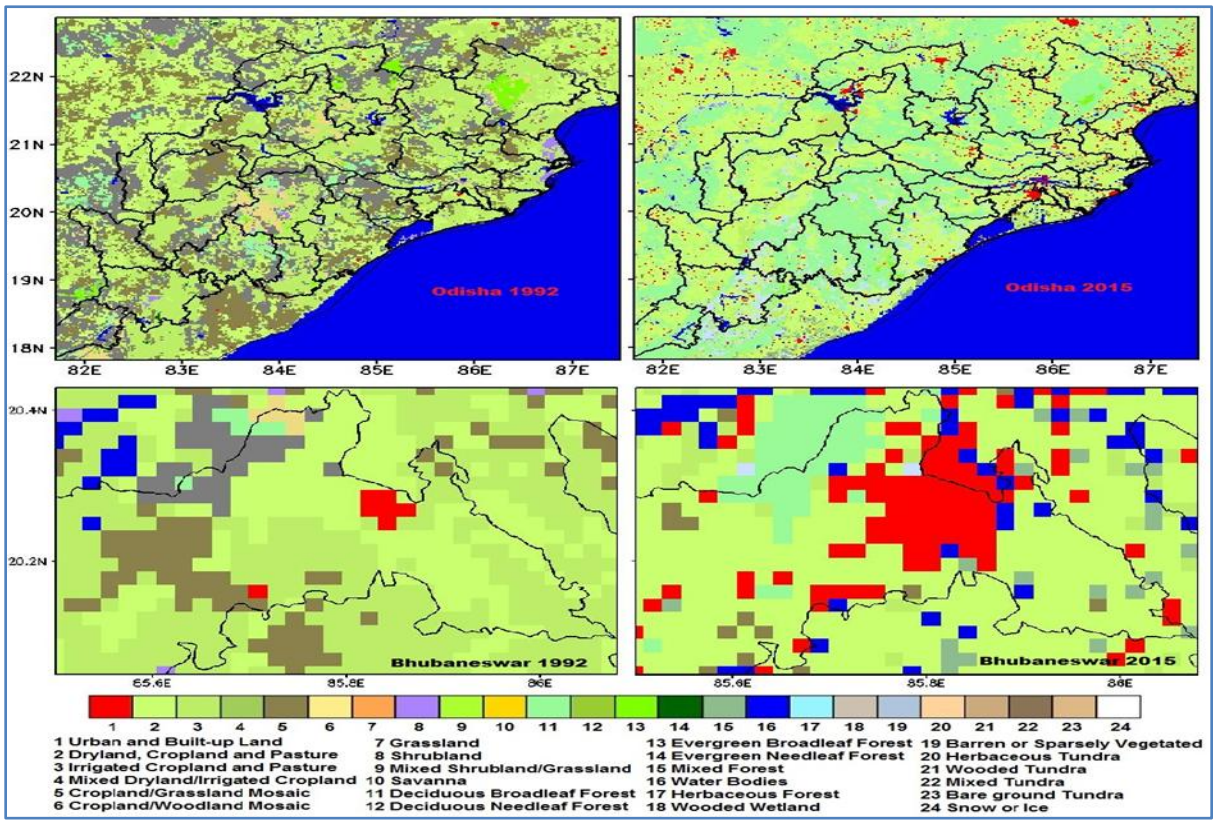

Fig. 4. Spatial distribution of model-simulated land-use map of Odisha (Upper Panel), and over Bhubaneswar (lower panel) during the event period using USGS (left Panel) and ISRO (right panel)

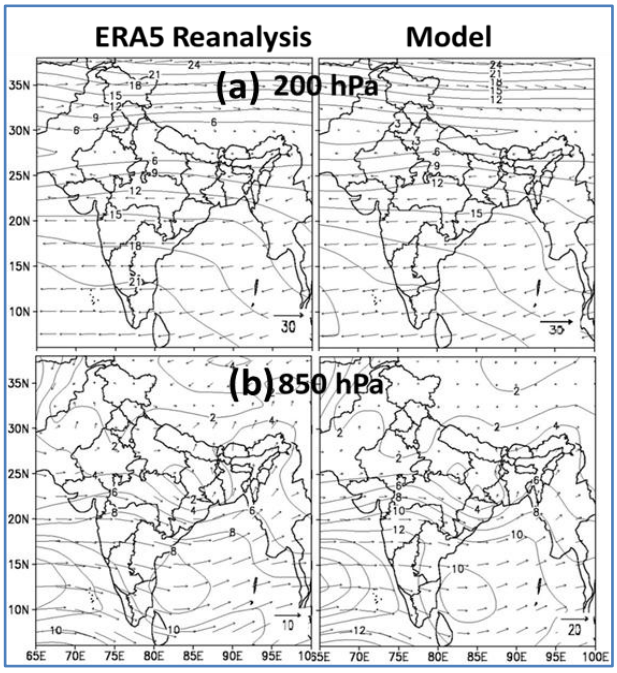

Figs. 5(a&b). Average wind circulation pattern for (a) 200hPa (upper panel) and (b) 850 hPa (bottom panel) from ERA5 Reanalysis(left) and the Model simulation (right) during the event period

spatial distribution of maximum temperature from ERA5 and the model (left to right) using two different data sets are shown in Fig. 7. The results compare near-surface temperature over Odisha at 09 UTC for 25 May (top row) and 26 May 2015 (bottom row) using observations/ reanalysis and two model experiments as represented in Fig. 7. From left to right, the panels show IMD observed maximum temperature (MaxT), ERA5 2-m temperature (t2m), the model control run, the model test run, and the difference MaxT as simulated by 2 experiments (*i.e.* test − control). Across both days, the spatial pattern highlights a hot inland region (dominantly warm/red shades) with a cooler coastal strip and localized cooler patches (blue shades), consistent with marine influence/sea-breeze modulation near the coast. The test and control temperature fields are broadly similar in large-scale structure, but the difference maps indicate that the model test configuration produces localized warming and cooling (up to about ±5 °C), with the strongest signals concentrated near the coastline and adjoining land–sea transition, reveals that the simulations from test experiments changes primarily affect surface energy balance and boundary-layer processes in coastal zones rather than uniformly across the domain.

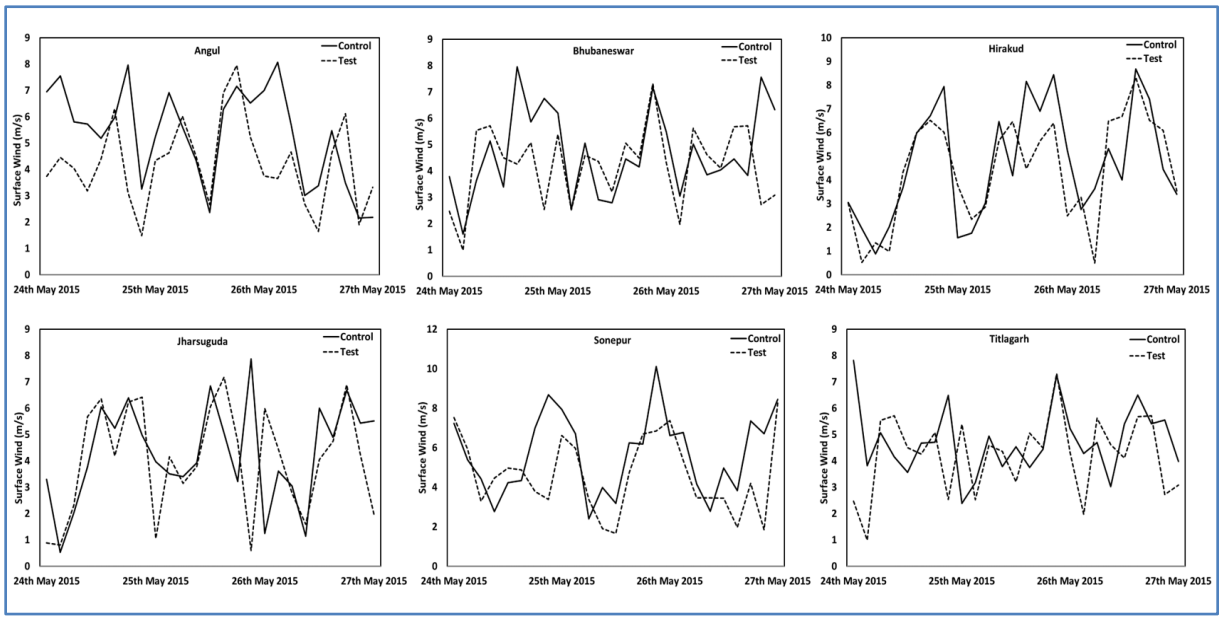

Fig. 6. Comparison of surface wind analysis at selected locations in Odisha from the control (solid line) and test (dashed line) simulations from 00UTC on 24th May 2015 to 00UTC on 27th May 2015

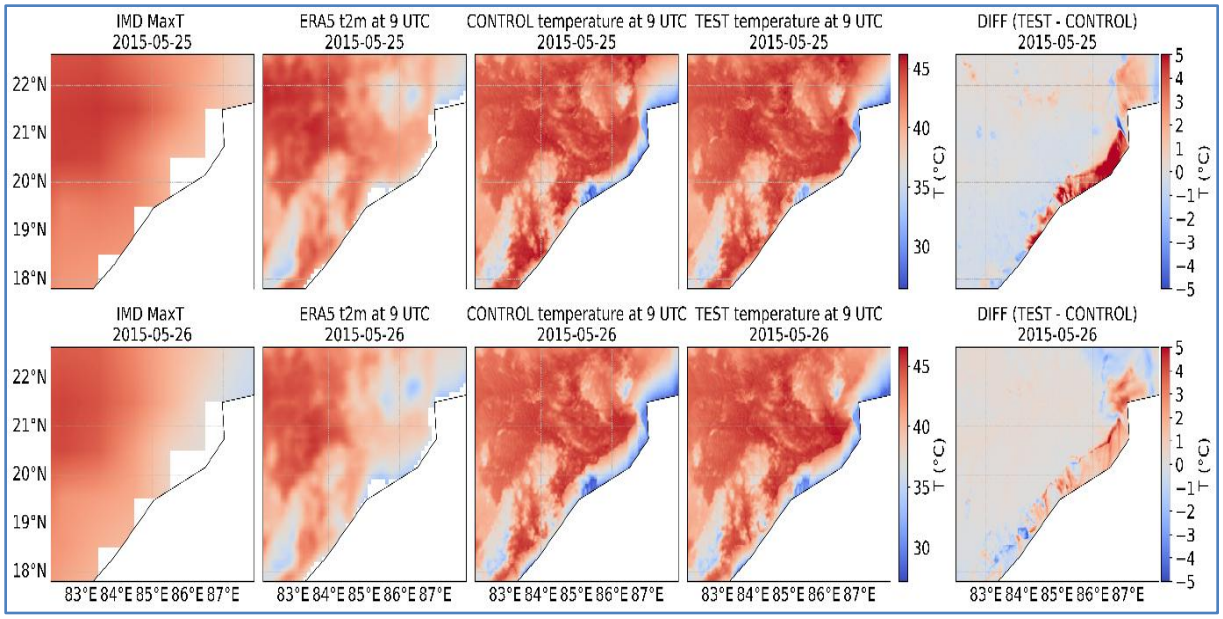

Fig.7. Comparison of maximum temperature (°C) observed from IMD, ERA5, and model simulations (control and test), and the differences of test and control simulations over Odisha on 25 (top panel) and 26 May 2015 (bottom panel)

The maximum temperatures for 25 and 26 May 2015 over the entire Odisha were simulated well and in close agreement with IMD station-scale observations (Tables 2 and 3), but not with ERA5 land, which shows maximum temperatures only over the western part of the state. The test simulation (more urbanized) shows that the station's maximum temperature is closer to the IMD station-scale observations due to land-use change, lower vegetation coverage resulting from increased anthropogenic activities, and altered local weather systems. The average absolute error in the maximum temperature of 19 meteorological stations with respect to the IMD station scale observations is 1.6 and 4.2 for the test, whereas3 and 4.7 for control simulations during

TABLE 2

The performance of the simulated maximum temperature (ºC) with IMD station scale observation was on 25 May 2015

Locations	IMD Station Observation (*ºC*)	Model Simulation (*ºC*)		Absolute Error (%)	
		Control	Test	Control	Test
Angul	47	45.8	46.43	2.55	1.21
Balasore	35.6	33.6	34.5	5.62	3.09
Baripada	40	38.9	40.7	2.75	1.75
Bhawanipatna	45.2	43.6	45.03	3.54	0.38
Bhubaneswar	45.4	44.52	44.87	1.94	1.17
Bolangir	46.2	45.32	45.99	1.90	0.45
Chandbali	41.9	40.7	41.4	2.86	1.19
Cuttack	41.6	39.98	42	3.89	0.96
Gopalpur	33.1	32.5	33.56	1.81	1.39
Hirakud	46.6	43.54	43.89	6.57	5.82
Jharsuguda	46.4	44.15	44.97	4.85	3.08
Keonjhar	42.3	42.1	43	0.47	1.65
Malkangiri	43.4	42.2	43.07	2.76	0.76
Phulbani	42.2	40.67	41.56	3.63	1.52
Sambalpur	46.4	45.3	46.13	2.37	0.58
Sonepur	43.9	44.21	44.28	0.71	0.87
Sundargarh	45	43.9	44.91	2.44	0.20
Talcher	45.1	43.89	44.23	2.68	1.93
Titilagarh	46.5	45.06	45.18	3.10	2.84
Avg. over all Stations	**43.36**	**42.10**	**42.93**	**2.97**	**1.62**

TABLE 3

The performance of the simulated maximum temperature (ºC) with IMD station scale observation was on 26 May 2015

Locations	IMD Station Observation (*ºC*)	Model Simulation (*ºC*)		Absolute Error (%)	
		Control	Test	Control	Test
Angul	45.1	43.8	43.91	2.88	2.64
Balasore	35.4	37.9	38.2	7.06	7.91
Baripada	38	40	40.2	5.26	5.79
Bhawanipatna	45.7	43.8	44.1	4.16	3.50
Bhubaneswar	39.8	41.95	42.12	5.40	5.83
Bolangir	46	44.19	44.32	3.93	3.65
Chandbali	38.8	40.2	39.4	3.61	1.55
Cuttack	37.4	40.8	41.5	9.09	10.96
Gopalpur	33.1	38.4	37.45	16.01	13.14
Hirakud	46.6	43.98	44.65	5.62	4.18
Jharsuguda	46	43.67	44.32	5.07	3.65
Keonjhar	39.5	40.1	40.21	1.52	1.80
Malkangiri	42	43.05	42.76	2.50	1.81
Phulbani	42.8	43.65	42.98	1.99	0.42
Sambalpur	46.4	43.94	44.67	5.30	3.73
Sonepur	45.2	44.31	43.94	1.97	2.79
Sundargarh	44.5	43.56	43.89	2.11	1.37
Talcher	42.2	42.32	42.47	0.28	0.64
Titilagarh	47.6	44.78	45.63	5.92	4.14
Avg of all Stations	**42.22**	**42.34**	**42.46**	**4.72**	**4.18**

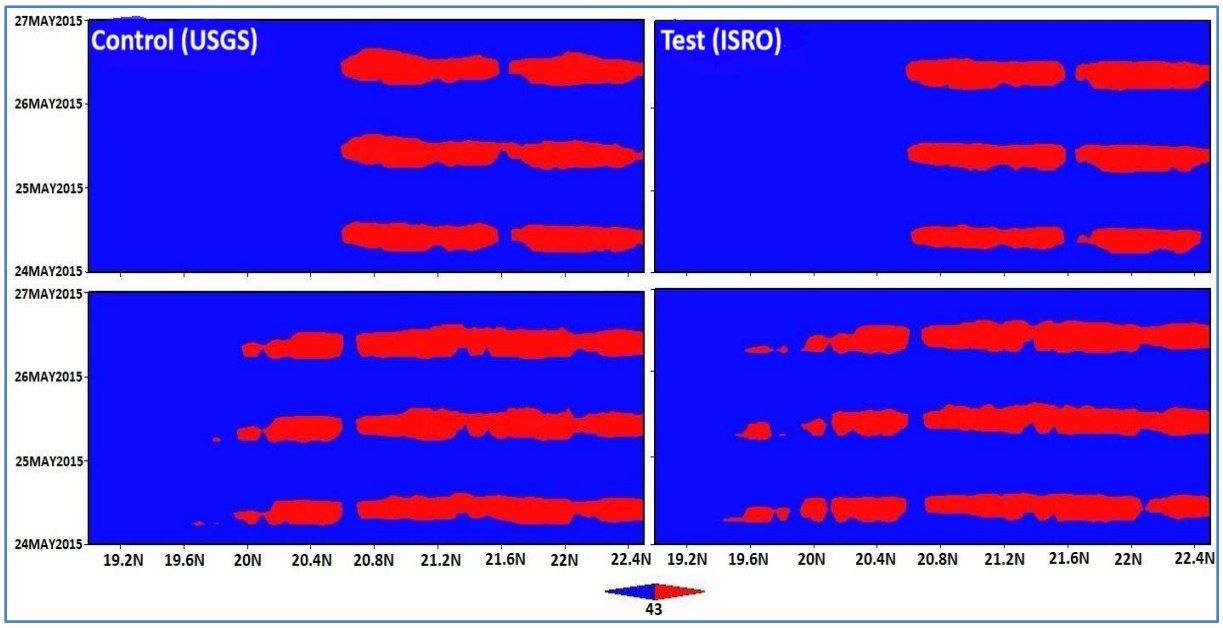

Fig. 8. Latitudinal distribution of maximum temperatures (ºC) on different days (y-axis) for the fixed longitude (84 °E, top panel, and 85 °E, bottom panels). The left and right panels present Control (USGS) and Test (ISRO) simulations

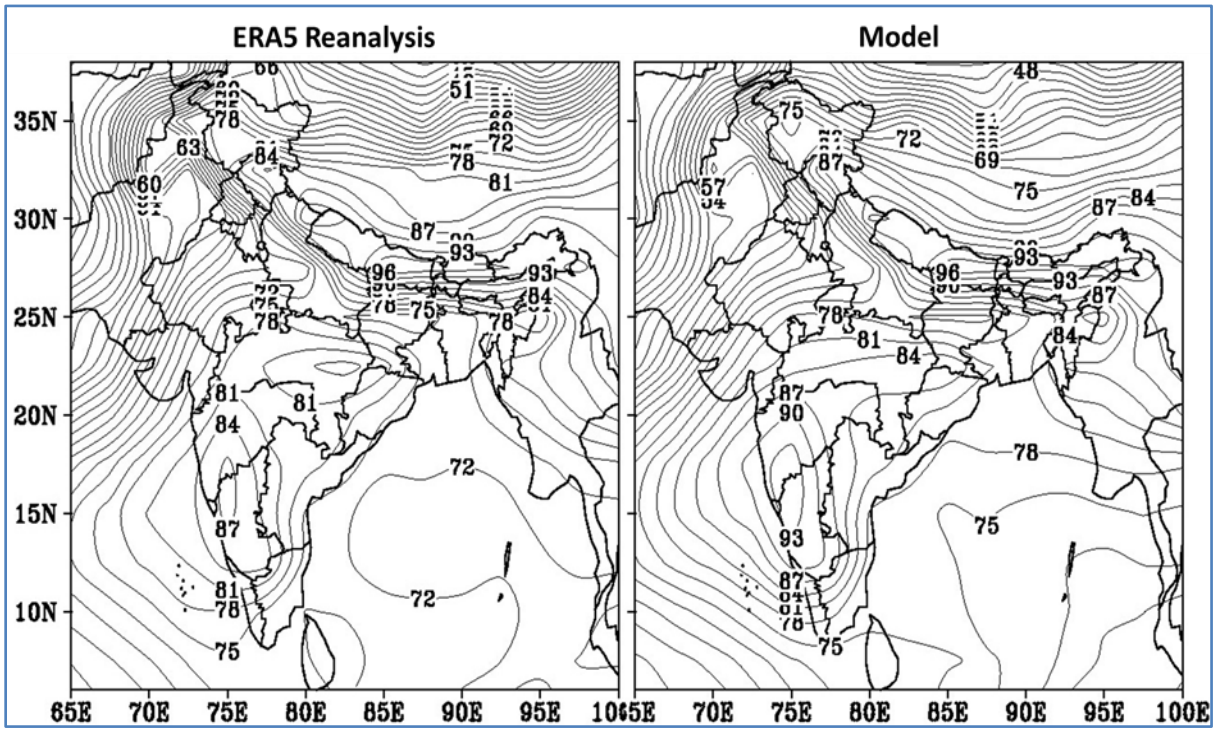

Fig. 9. Average relative humidity (%) during the heat wave period (24-27 May 2015) from the ERA5 Reanalysis (left) and Model simulation (right)

the 25th and 26th May 2015. From this analysis, it can be concluded that the ISRO-observed land-use data provides a realistic portrayal of the land-use scenario (more urbanized) and results in a more accurate simulation of extreme temperatures (heat waves).

Two sets of land use data were analyzed to determine the predicted maximum temperature for the three-day simulation period. The Latitude-time plots averaged along fixed longitudes (84 °C, top panel; 85 °C, bottom panel) for both test and control simulations are shown in Fig. 8, where

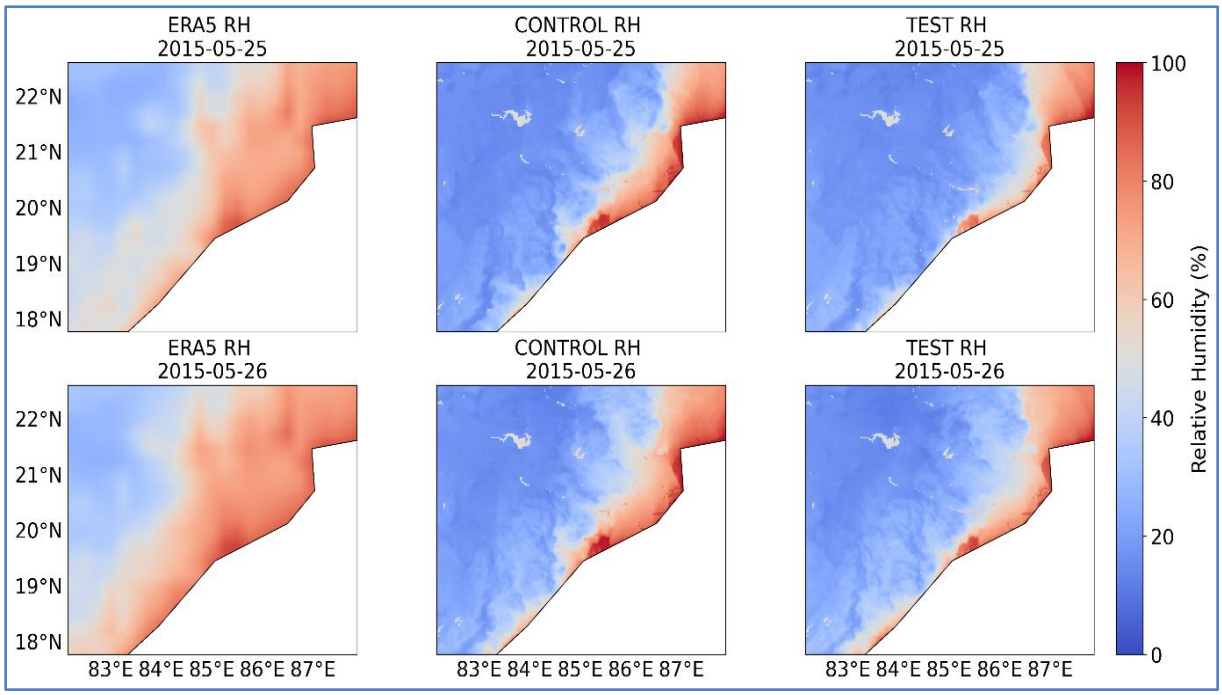

Fig. 10. Comparison of daily averaged relative humidity (%) during 24 and 25 May 2015 from the ERA5 Reanalysis (left) and Model simulations (control: middle panel and test: right panel)

most stations observed more than 45. The spatial and temporal extent of the maximum temperature is presented in this figure. The study shows that an extreme temperature exceeding 43 °C is spatially (20–22 °N) and temporally (approximately 4–6 hours per day) along 84–85 °E. A more extended (5–6 h) period of extreme temperature was observed on May 25, 2015, in all of the simulations along 85 °E. This figure shows the prolonged maximum temperatures across western and central Odisha, which caused the heat wave.

3.5. *Relative humidity analysis*

An increase in vegetation and forest cover generally increases atmospheric moisture content through evapotranspiration, thereby increasing relative humidity. From the above discussion, coastal Odisha experiences lower temperature rises than western Odisha, which could be due to differences in humidity levels across the regions. The comparison between the observation and model simulation of relative humidity is presented in Fig. 9. The coastal district exhibits more relative humidity than the western part of Odisha in the observation and model simulation, thus signifying that the surface moisture is sensitive to altered physics, land surface processes, or boundary-layer processes in the model test configuration. The maximum temperature in western Odisha was higher than in the state's coastal region. Fig. 10 represents the relative humidity (RH, %) over Odisha for 25 May (top row) and 26 May 2015 (bottom row). The ERA5 (left column) reanalysis is compared with the model simulations, *i.e*., control (middle) and test (right). On both days, ERA5 analysis indicates a broad west–east humidity gradient, with higher RH toward the coastal/northeastern side and drier air inland. The model simulations reproduce the key spatial structure, showing a pronounced high-RH coastal belt (moist marine influence/sea-breeze zone) and lower RH inland, consistent with stronger land heating and deeper mixing. Differences between the test and control simulations are subtle at the large-scale, but the test simulation slightly alters the strength and inland.

3.6. *Outgoing longwave radiation analysis*

Heat-wave episodes are commonly associated with persistent anticyclonic circulation and mid-tropospheric subsidence that suppresses cloud development; this reduced cloudiness is reflected in positive outgoing longwave radiation (OLR) anomalies, consistent with clearer skies and stronger surface heating (Rohini *et al*., 2016). Over India, heat-wave variability is further modulated by large-scale tropical dynamics: different MJO phases influence heat-wave intensity, duration, and frequency, and these linkages are often diagnosed using OLR composites (Devi *et al*., 2024). Because heat-wave characteristics vary strongly across plains, coastal zones, and hilly terrain, region-specific thresholds are needed to represent spatial patterns and emerging hotspots robustly (Devi *et al*., 2023). Process-based temperature-tendency diagnostics also show that hot extremes are sustained by a

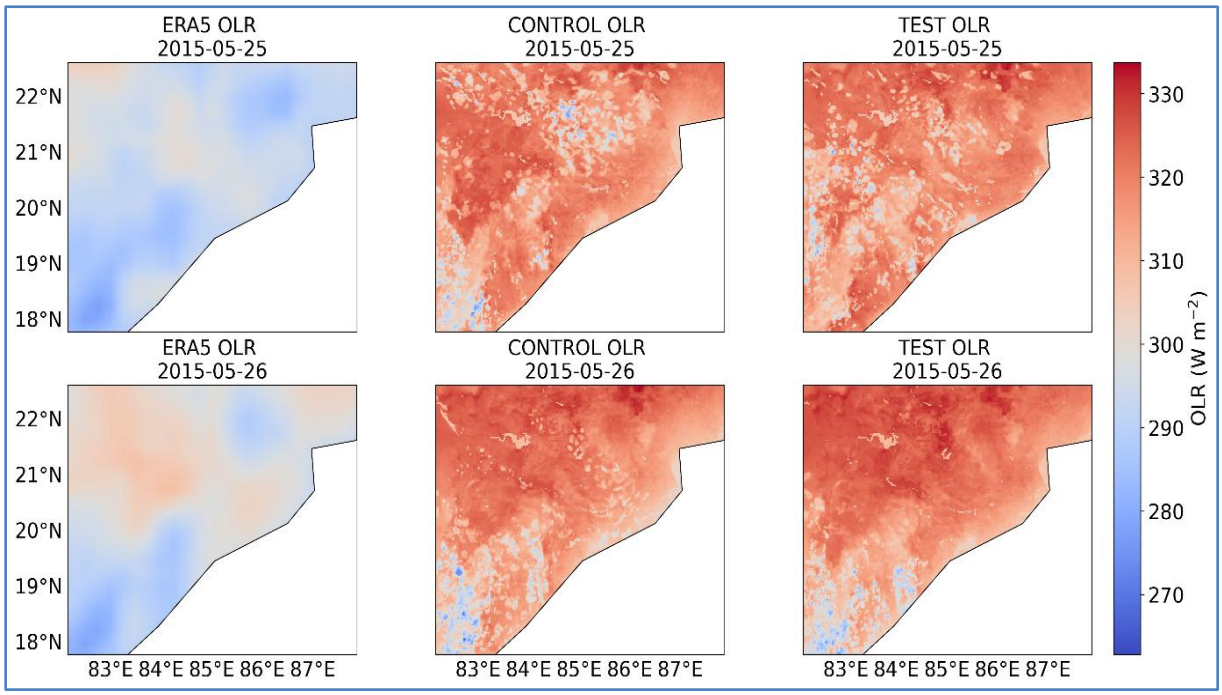

Fig. 11. Comparison of daily averaged OLR (W/m^2) during 24 and 25 May 2015 from the ERA5 Reanalysis (left) and Model simulations (control: middle panel and test: right panel)

balance of dynamical and diabatic terms, with diabatic heating explicitly incorporating an OLR-related component alongside radiative, latent, and turbulent contributions (Devi *et al*., 2024). It was found that during the heat-wave periods considered in the present study, the wind speed was approximately 7-8 m/s according to ERA5 reanalysis data. Fig. 11 compares the outgoing longwave radiation (OLR, W m^{-2}) for 25 May (top row) and 26 May 2015 (bottom row) from ERA5 (left) and the model CONTROL and TEST runs (middle and right). Overall, the domain is dominated by high OLR (~310–330 W m^{-2}) in the model fields, which indicates clear skies, strong surface warming, and suppressed deep convection-a thermodynamic setup consistent with heat - wave conditions. The lower OLR pockets (cooler/bluish shades) indicate areas of enhanced cloudiness or deeper convection, where cloud-top temperatures are colder, leading to reduced OLR. Compared with the model control run, the test simulation shows modest spatial changes in OLR, mainly by slightly shifting or adjusting the extent/intensity of the low-OLR (cloudy/convective) patches, implying that the model test configuration modifies cloud–radiation interactions and convective activity more than it change the broad synoptic-scale clear-sky background. The sharp increase in the maximum temperature during the event appears to have been driven by the high OLR and the absence of convection; a persistently dry, arid wind typically worsens these events.

3.7. *CAPE/CIN analysis*

The convective state is succinctly described by CAPE, which quantifies the energy available for buoyant updrafts, and CIN, which represents the inhibition (cap) that must be overcome for convection to initiate. When CIN is elevated, storm initiation is suppressed, allowing heat to persist and, in some cases, permitting CAPE to accumulate without being released through deep convection (Myoung and Nielen, 2010; Langenbrunner, 2020). In this study, the CAPE/CIN analysis was also carried out using ERA5 and model simulations. Fig. 12 shows the CAPE and CIN variations over Odisha for 25 May and 26 May 2015, comparing ERA5 (left column) with the model control (middle) and test (right). ERA5 (CAPE, J kg^{-1}; Top two rows) shows a strong coast-inland gradient, with higher CAPE toward the eastern/northeastern region and lower values inland. Both the simulation experiments reproduce the key feature of a CAPE-enhanced coastal belt, consistent with moist marine air and boundary-layer convergence near the coast that can support convection if triggered. The CIN (J kg^{-1}; bottom two rows) indicates where convection is suppressed by a cap (stronger inhibition) versus where parcels can more easily reach free convection (weaker inhibition). The model runs show broader, more spatially continuous CIN patterns than ERA5, suggesting differences in boundary-layer stability and capping strength. The model (test run) produces small but coherent shifts in the extent/ intensity of the coastal

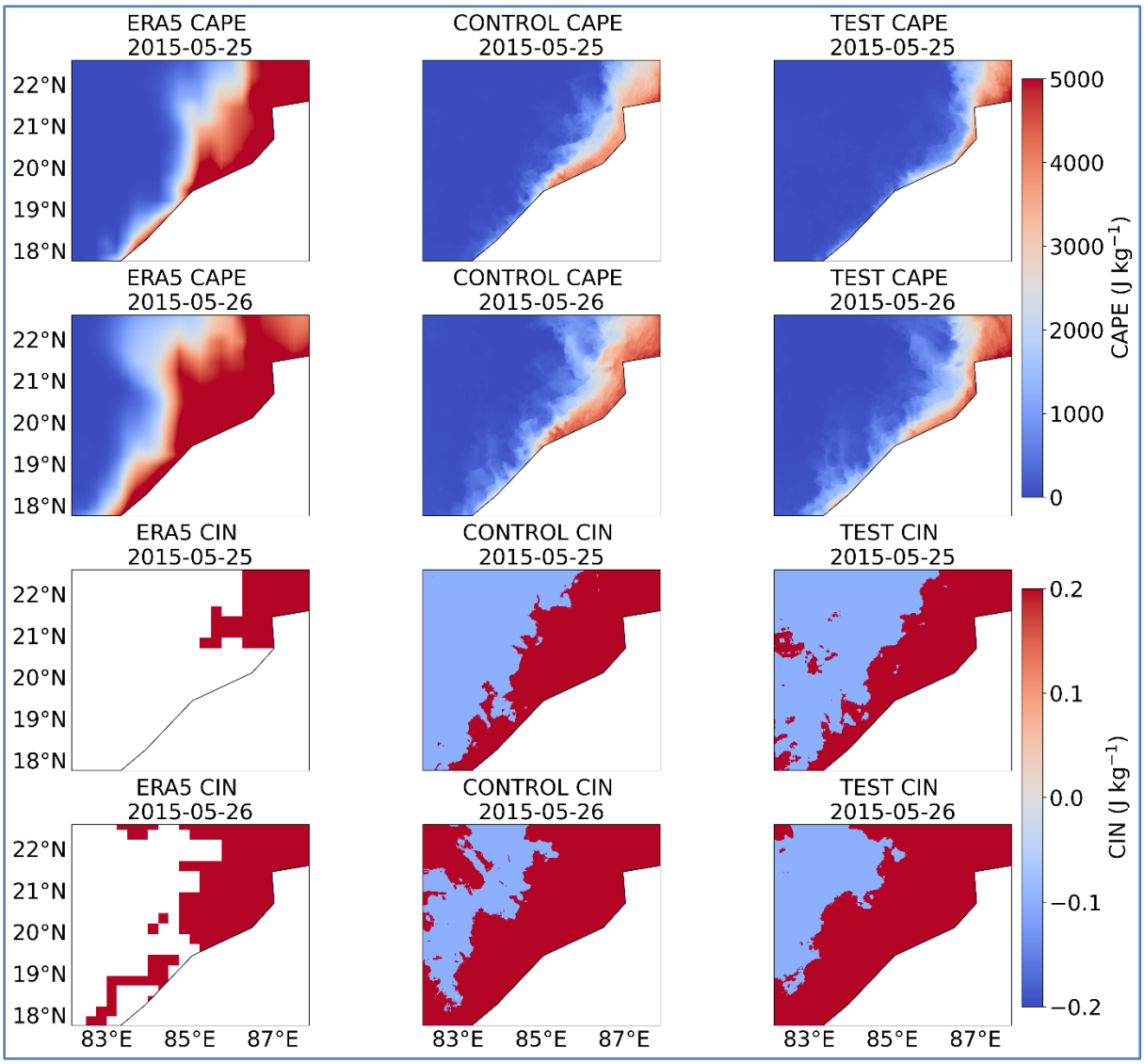

Fig. 12. Comparison of daily averaged CAPE (top two panels) and CIN (bottom two panels) expressed in J kg⁻¹ during 24 and 25 May 2015 from the ERA5 Reanalysis (left) and Model simulations (control: middle panel and test: right panel)

CAPE zone and in the distribution of CIN, meaning the model test configuration slightly modifies the balance between available instability (CAPE) and suppression (CIN)-and therefore the likelihood of convection initiation-especially along the coastal transition zone.

4. Conclusions

The last week of May 2015 experienced comparatively extreme temperatures across most regions of Odisha, with temperatures exceeding 47 °C in several locations, notably western and central Odisha. The state experienced a severe heat wave for two weeks due to an unexpected rise in temperatures. The IMD declared May 25–27 as a "red box zone" after the maximum temperatures in eight major cities exceeded 45 °C. This study was based on observational analysis and model simulations using two land-use datasets (USGS and ISRO), covering the period from 1992 to 2015. This study confirms previous work (Srivastava *et al.*, 2014) that indicates an increase in hot days per decade (5.1 days) and a significant increase in daily maximum temperatures throughout Odisha. The important findings of the study are discussed below:

The maximum temperature trend for the study period (1969–2015) likewise shows a positive value (0.04 °C/year), whereas during the last decade (2009-15) it rose at a rate of 0.41 °C/year. The massive change in maximum temperature across the coastal districts and the state is due to changes in land-use patterns, as suggested by Gogoi et al. (2019) and our land-use analysis plot. LULC changes and urbanization are driving summer (May)

temperatures in Odisha higher, contributing to the severity of heat waves.

The most recent land-use data also show the emergence of numerous new, dispersed urban built-up patches throughout the state. So, urban expansion and land-use change over time reduce vegetation due to anthropogenic activities, affecting local weather systems and intensifying heat waves.

Surface wind decreases due to higher surface roughness, which can increase wind shear and thus enhance turbulent mixing in the boundary layer. This suggests a more realistic representation of the urban landscape in the latest ISRO land-use data compared to older USGS datasets.

The intensity and spatial pattern of intense temperatures across various regions, such as the western and central parts of Odisha, are successfully simulated by the WRF model, along with associated parameters such as RH and OLR, and thermodynamic indices such as CAPE and CIN. There is also reasonable agreement in simulated and observed temperature over the two days shown in the figure, which clearly indicates that the maximum temperature over the state from simulation (more urbanized) and observation are closer than in less urbanized. The average absolute error in maximum temperature of 19 meteorological stations w.r.t IMD station scale observation is 1.6% and 4.2% for the test (more urbanized), whereas 3% and 4.7% for control (less urbanized) simulations during the 25th and 26th May 2015. There was a heat wave across the state due to an extended period of elevated maximum temperatures (5–6 hours), as shown in the latitudinal temperature distribution. This phenomenon is also evident in different parts of western and central Odisha.

The coastal district exhibits higher relative humidity than the western part of Odisha in both observations and model simulations, indicating that the maximum temperature over the western part of Odisha was higher than that over the Coastal part.

The WRF model configuration presented in the could able to simulate the extreme temperature (heat wave episode) with different land use from USGS and ISRO, showing that the model is vulnerable to land use change, representing realistic urban scenarios (ISRO) that can be used for advanced forecasts of such heatwave events with reasonable and actionable confidence. The limitations of the study demand an ensemble modeling approach and a better representation of parameterization schemes, along with a sustained high-resolution observational network for improved validation. An early warning of such events is essential due to the significance of extreme temperatures, the primary cause of heat-wave conditions, and the health risk (like heat strokes) to humans and animals.

Availability of data and material

Data analysis codes are available from the corresponding author upon reasonable request.

Conflict of interest

The authors declare that they have no known competing interests

Funding

This work is supported by the projects funded by the National Mission on Himalayan Studies (NMHS) of the Ministry of Environment, Forest and Climate Change (MoEFCC), Govt. of India, for the project funding support (grant no: GBPNI/NMHS-2019-20/MG/315).

Author's Contribution

SK Sahoo: Conceptualization, analysis, investigation, and original and final draft preparation (*email: sanjeeb@ncmrwf.gov.in*).
KC Gouda: Conceptualization, Supervision, Final Draft preparation (*email: kcgouda@csir4pi.in*).
S Himeash: Conceptualization, Supervision, and Final draft preparation (*email: snehii@yahoo.com*).
RK Sahu: Analysis and Investigation (*email: rsahu657@gmail.com*).

Acknowledgements

The authors sincerely acknowledge the Department of Science and Technology, Government of India, for funding initiatives (SB/S4/AS-113/2013, SB/S4/AS-120/2014, and INT/RUS/RFBR/P-336). The authors also acknowledged the Head of CSIR 4PI for their encouragement and support. We kindly acknowledge the use of the CSIR 4PI high-performance computing (HPC) facility for computational work.

Disclaimer: The contents and views expressed in this research article are the views of the authors and do not necessarily reflect the views of the organizations they belong to.

References

Beuria, R., Sahu, D., Sahu, S. C., *et al.*, 2025, "Heatwave-Induced Thermoregulatory Stress in Odisha's Coastal and North-Eastern

Districts: Examining the April 2024 Event Using Advanced Statistical and Geospatial Techniques", Dynamics of Atmospheres and Oceans, 101577. doi: https://doi.org/10.1016/j.dynatmoce.2025.101577.

Black, E., Blackburn, M., Harrison, G., Hoskins, B., and Methven, J., 2004, "Factors contributing to the summer 2003 European heatwave", *Weather*, **59**, 217–223. doi: https://doi.org/10.1256/wea.74.04.

Chung, U., Choi, J., and Yun, J. I., 2004, "Urbanization Effect on the Observed Change in Mean Monthly Temperatures between 1951–1980 and 1971–2000 in Korea", *Climatic Change*, **66**, 127–136. doi: https://doi.org/10.1023/B:CLIM.0000043136.58100.ce.

Dasari, H. P., Salgado, R., Perdigao, J., and Challa, V. S., 2014, "A Regional Climate Simulation Study Using WRF-ARW Model over Europe and Evaluation for Extreme Temperature Weather Events", *International Journal of Atmospheric Sciences*, **2014**, 1–22. doi: https://doi.org/10.1155/2014/704079.

De, U. S., and Mukhopadhyay, R.K., 1998, "Severe heat wave over Indian subcontinent in 1998 in a perspective of global climate", *Current Science*, **75**, 1308–1311. doi: http://www.jstor.org/stable/24101015.

De, U.S., and Sinha Ray, K.C., 2000, "Weather and Climate impacts on health in mega cities," *WMO Bulletin*, **44**, pp. 340–348.

Devi, R., Gouda, K. C., and Lenka, S., 2023, "Analysis of heat wave over different physiographical regions in India", *Theoretical and Applied Climatology*, **154**, 1343–1356. doi: https://doi.org/10.1007/s00704-023-04639-2.

Devi, R., Gouda, K.C. and Lenka, S., 2024, "Assessment of long-term spatio-temporal variability of hot extremes and associated physical mechanism over India", *Stochastic Environmental Research and Risk Assessment*, **38**, 3257–3272. doi: https://doi.org/10.1007/s00477-024-02744-w.

Dudhia, J., 1989, "Numerical Study of Convection Observed during the Winter Monsoon Experiment Using a Mesoscale Two-Dimensional Model", *Journal of the Atmospheric Sciences*, **46**, 3077–3107. doi: https://doi.org/10.1175/1520-0469(1989)046<3077:NSOCOD>2.0.CO;2.

Fan, C., Myint, S. W., Kaplan, S., *et al*., 2017, "Understanding the Impact of Urbanization on Surface Urban Heat Islands—A Longitudinal Analysis of the Oasis Effect in Subtropical Desert Cities", *Remote Sensing*, **9**, 672. doi: https://doi.org/10.3390/rs9070672.

Fink, A. H., Brücher, T., Krüger, A., Leckebusch, G. C., Pinto, J. G., and Ulbrich, U., 2004, "The 2003 European summer heatwaves and drought –synoptic diagnosis and impacts", *Weather*, **59**, 209–216. doi: https://doi.org/10.1256/wea.73.04.

Fujibe, F., 2008, "Detection of urban warming in recent temperature trends in Japan", *International Journal of Climatology*, **29**, 1811–1822. doi: https://doi.org/10.1002/joc.1822.

García-Díez, M., Fernández, J., and Vautard, R., 2015, "An RCM multi-physics ensemble over Europe: multi-variable evaluation to avoid error compensation", *Climate Dynamics*, **45**, 3141–3156. doi: https://doi.org/10.1007/s00382-015-2529-x.

Gershunov, A., Cayan, D. R., and Iacobellis, S. F., 2009, "The Great 2006 Heat Wave over California and Nevada: Signal of an Increasing Trend", *Journal of Climate*, **22**, 6181–6203. doi: https://doi.org/10.1175/2009JCLI2465.1.

Gharai, B., Rao, P. V. N., and Dutt, C. B. S., 2018, "Mesoscale Model Compatible IRS-P6 AWiFS-Derived Land use/Land Cover of Indian Region", *Current Science*, **115**, 2301. doi: https://doi.org/10.18520/cs/v115/i12/2301-2306.

Gogoi, P. P., Vinoj, V., Swain, D., Roberts, G., Dash, J., and Tripathy, S., 2019, "Land use and land cover change effect on surface temperature over Eastern India", *Scientific Reports*, **9**, 8859. doi: https://doi.org/10.1038/s41598-019-45213-z.

Goswami, P., Shivappa, H., and Goud, B. S., 2010, "Impact of urbanization on tropical mesoscale events: investigation of three heavy rainfall events", *Meteorologische Zeitschrift*, **19**,385–397. doi: https://10.1127/0941-2948/2010/0468.

Gouda, K. C., Sahoo, S. K., Samantray, P., and Himesh, S., 2017, "Simulation of extreme temperature over Odisha during May 2015", *Weather and Climate Extremes*, **17**,17–28. doi: https://doi.org/10.1016/j.wace.2017.07.001.

Grell, G. A. and Dévényi, D., 2002, "A generalized approach to parameterizing convection combining ensemble and data assimilation techniques", *Geophysical Research Letters*, **29**(14), doi: https://10.1029/2002GL015311.

Grover, A. and Singh, R., 2015, "Analysis of Urban Heat Island (UHI) in Relation to Normalized Difference Vegetation Index (NDVI): A Comparative Study of Delhi and Mumbai", *Environments*, **2**, 125–138. doi: https://doi.org/10.3390/environments2020125.

Halder, S., Saha, S. K., Dirmeyer, P. A., *et al.*, 2016, "Investigating the impact of land-use land-cover change on Indian summer monsoon daily rainfall and temperature during 1951–2005 using a regional climate model", *Hydrology and Earth System Sciences*, **20**, 1765–1784. doi: https://doi.org/10.5194/hess-20-1765-2016.

Hong, S. Y. and Lim, J.-O. J., 2006, "The WRF Single-Moment 6-Class Microphysics Scheme (WSM6)", *Asia-Pacific Journal of Atmospheric Sciences*, **42**,129–151. doi: https://10.1007/BF02945806.

Hong, S.-Y., Noh, Y., and Dudhia, J., 2006, "A New Vertical Diffusion Package with an Explicit Treatment of Entrainment Processes", *Monthly Weather Review*, **134**, 2318–2341. doi: https://10.1175/MWR3199.1.

Hulme, M., Zhao, Z.-C., and Jiang, T., 1994, "Recent and future climate change in east asia", *International Journal of Climatology*, **14**, 637–658. doi: https://doi.org/10.1002/joc.3370140604.

IPCC., 2007, "Climate Change 2007."

Jalan, S. and Sharma, K., 2014, "Spatio-temporal Assessment of Land Use/ Land Cover Dynamics and Urban Heat Island of Jaipur City using Satellite Data", T*he International Archives of the Photogrammetry, Remote Sensing and Spatial Information Sciences*, **XL–8**, 767–772. Doi: https://doi.org/10.5194/isprsarchives-XL-8-767-2014.

Jiang, Y., Fu, P., and Weng, Q., 2015, "Assessing the Impacts of Urbanization-Associated Land Use/Cover Change on Land Surface Temperature and Surface Moisture: A Case Study in the Midwestern United States", *Remote Sensing*, **7**, 4880–4898. doi: https://10.3390/rs70404880.

Kumar, R., Mishra, V., Buzan, J., Kumar, R., Shindell, D., and Huber, M., 2017, "Dominant control of agriculture and irrigation on urban heat island in India", *Scientific Reports*, **7**, 14054. doi: https://10.1038/s41598-017-01408-2.

Langenbrunner, B., 2020, "Trouble rising", *Nature Climate Change*, **10**, 100–100. doi: https://doi.org/10.1038/s41558-020-0701-8.

Lau, N.-C. and Nath, M. J., 2012, "A Model Study of Heat Waves over North America: Meteorological Aspects and Projections for the

Twenty-First Century", *Journal of Climate*, **25**, 4761–4784. doi: https://doi.org/10.1175/JCLI-D-11-00575.1.

Li, D., Sun, T., Liu, M., Yang, L., Wang, L., and Gao, Z., 2015, "Contrasting responses of urban and rural surface energy budgets to heat waves explain synergies between urban heat islands and heat waves", *Environmental Research Letters*, **10**, 054009. doi: https://10.1088/1748-9326/10/5/054009.

Li, Q., Zhang, H., Liu, X., and Huang, J., 2004, "Urban heat island effect on annual mean temperature during the last 50 years in China", *Theoretical and Applied Climatology*, **79**,165–174. doi: https://doi.org/10.1007/s00704-004-0065-4.

Loveland, T. R., Reed, B. C., Brown, J. F., *et al*., 2000, "Development of a global land cover characteristics database and IGBP DISCover from 1 km AVHRR data", *International Journal of Remote Sensing*, **21**, 1303–1330. doi: https://doi.org/10.1080/014311600210191.

Mahato, A., Satyanarayana, A.N.V., 2025, "Climatological Analysis in Identification of Pre-monsoon Convective Potential Zones over Eastern and North-Eastern States of India During the Last Four Decades". *Pure Appl. Geophys*. **182**, 3005–3032. doi: https://doi.org/10.1007/s00024-025-03743-w.

Mbokodo, I., Bopape, M. J., Chikoore, H., Engelbrecht, F., and Nethengwe, N. 2020, "Heatwaves in the future warmer climate of South Africa", *Atmosphere*, **11**, 712. doi: https://doi.org/10.3390/atmos11070712.

Mlawer, E. J., Taubman, S. J., Brown, P. D., Iacono, M. J., and Clough, S. A., 1997, "Radiative transfer for inhomogeneous atmospheres: RRTM, a validated correlated-k model for the longwave", *Journal of Geophysical Research Atmospheres*, **102**, 16663–16682. doi: https://10.1029/97JD00237.

Mohan, M. and Kandya, A., 2015, "Impact of urbanization and land-use/land-cover change on diurnal temperature range: A case study of tropical urban airshed of India using remote sensing data", *The Science of the Total Environment*, **506–507**, 453–465. doi: https://10.1016/j.scitotenv.2014.11.006.

Mohan, M., Kandya, A., and Battiprolu, A., 2011, "Urban Heat Island Effect over National Capital Region of India: A Study using the Temperature Trends", *Journal of Environmental Protection*, **02**, 465–472. doi: https://10.4236/jep.2011.24054.

Mohan, M., Kikegawa, Y., Gurjar, B. R., Bhati, S., Kandya, A., and Ogawa, K., 2012, "Urban Heat Island Assessment for a Tropical Urban Airshed in India", *Atmospheric and Climate Sciences*,**02**, 127–138. doi: https://10.4236/acs.2012.22014.

Mooney, P. A., Mulligan, F. J., and Fealy, R., 2013, "Evaluation of the Sensitivity of the Weather Research and Forecasting Model to Parameterization Schemes for Regional Climates of Europe over the Period 1990–95", *Journal of Climate*, **26**, 1002–1017. doi: https://doi.org/10.1175/JCLI-D-11-00676.1.

Myoung, B. and Nielsen-Gammon, J.W., 2010, "Sensitivity of monthly convective precipitation to environmental conditions", *Journal of Climate*, **23**,166–188. doi: https://10.1175/2009JCLI2792.1.

Nayak, S. and Mandal, M., 2019, "Impact of land use and land cover changes on temperature trends over India", *Land Use Policy*, **89**, 104238. https://doi.org/10.1016/j.landusepol.2019.104238.

Nayak, S., and Mandal, M., 2012, "Impact of land-use and land-cover changes on temperature trends over Western India", *Current Science*, **102**, 1166–1173. doi: https://www.jstor.org/stable/24107759.

Niyogi, D., Pyle, P., Lei, M., *et al*., 2011, "Urban Modification of Thunderstorms: An Observational Storm Climatology and Model Case Study for the Indianapolis Urban Region", *Journal of Applied Meteorology and Climatology*, **50**, 1129–1144. doi: https://doi.org/10.1175/2010JAMC1836.1.

Pai, D. S., Nair, S., and Ramanathan, A. N., 2013, "Long term climatology and trends of heat waves over India during the recent 50 years (1961-2010)", *Mausam*, **64**, 585–604. doi: https://doi.org/10.54302/mausam.v64i4.742.

Pai, D. S., Thapliyal, V., and Kokate, P. D., 2004, "Decadal variation in the heat and cold waves over India during 1971-2000", *Mausam*, **55**,281–292. doi: https://doi.org/10.54302/mausam.v55i2.1083.

Pandey, S. K., Vinoj, V., Landu, K., and Babu, S. S., 2017, "Declining pre-monsoon dust loading over South Asia: Signature of a changing regional climate", *Scientific Reports*, **7**. doi: https://doi.org/10.1038/s41598-017-16338-w.

Rao, P., Gupta, K., Roy, A. and Balan, R., 2021, "Spatio-temporal analysis of land surface temperature for identification of heat wave risk and vulnerability hotspots in Indo-Gangetic Plains of India. *Theoretical and Applied Climatology*, **146**, 567-582. doi: https://doi.org/10.1007/s00704-021-03756-0.

Ratnam, J. V., Behera, S. K., Ratna, S. B., Rajeevan, M., and Yamagata, T., 2016, "Anatomy of Indian heatwaves", *Scientific Reports*, **6**. doi: https://10.1038/srep24395.

Ren, G., Zhou, Y., Chu, Z., *et al*., 2008, "Urbanization Effects on Observed Surface Air Temperature Trends in North China", *Journal of Climate*, **21**,1333–1348. doi: https://10.1175/2007JCLI1348.1.

Rohini, P., Rajeevan, M. and Srivastava, A.K., 2016, "On the variability and increasing trends of heat waves over India", *Scientific reports*, **6**,1–9. doi: https://10.1038/srep26153.

Sahu, R., Tyagi, B., Vissa, N. and Mohapatra, M., 2022, "Pre-monsoon thunderstorm season climatology of convective available potential energy (CAPE) and convective inhibition (CIN) over eastern India", *Mausam*, **73**, 565–586. doi: https://10.54302/mausam.v73i3.1247.

Sahu, R.K., Dadich, J., Tyagi, B., Vissa, N.K. and Singh, J., 2020, "Evaluating the impact of climate change in threshold values of thermodynamic indices during pre-monsoon thunderstorm season over Eastern India", *Natural Hazards*, **102**, 1541–1569. doi: https://10.1007/s11069-020-03978-x.

Sahu, R.K., Nayak, S., Singh, K.S., Nayak, H.P. and Tyagi, B., 2023, "Evaluating the impact of topography on the initiation of Nor'westers over eastern India" *Geomatics, Natural Hazards and Risk*, **14**, 2184669. doi: https://10.1080/19475705.2023.2184669.

Sahu, R.K., Tyagi, B., Singh, K.S. and Nayak, H.P., 2024, "Evaluating the influence of the Shillong Plateau topography on thunderstorm activity over northeast India", *Pure and Applied Geophysics*, **181**, 1017–1038. doi: https://10.1007/s00024-024-03445-9.

Schär, C., Vidale, P. L., Lüthi, D., *et al*., 2004, "The role of increasing temperature variability in European summer heatwaves", *Nature*, **427**, 332–336. doi: https://10.1038/nature02300.

Sethi, B., Sahu, S.C., Gouda, K.C., Beuria, R., Mallick, M.K., Samal, S.K., Panigrahi, A. and Pati, A., 2025, "Climate variability and warming in Coastal Odisha: assessing interannual temperature trends and impacts", *Scientific Reports*, **15**, 11111. doi: https://10.1038/s41598-025-95035-5.

Singh, P., Kikon, N., and Verma, P., 2017, "Impact of land use change and urbanization on urban heat island in Lucknow city, Central India. A remote sensing based estimate", *Sustainable Cities and Society*, **32**, 10 doi: https://10.1016/j.scs.2017.02.0180–114.

Skamarock, C., Klemp, B., Dudhia, J., *et al*., 2019, "A Description of the Advanced Research WRF Model Version 4." *NCAR Technical Note* NCAR/TN-556+STR. doi: https://10.5065/1dfh-6p97.

Srivastava, A.K., Singh, G.P., Singh, O.P., *et al.*, 2014, "Recent variability and trends in temperatures over India", *Vayu Mandal*, **40**, 161–181.

Swain, D., Roberts, G. J., Dash, J., Lekshmi, K., Vinoj, V., and Tripathy, S., 2017, "Impact of Rapid Urbanization on the City of Bhubaneswar, India", *Proceedings of the National Academy of Sciences India Section a Physical Sciences*, **87**, 845–853. doi: https://10.1007/s40010-017-0453-7.

Tyagi, B., Sahu, R.K., Hari, M. and Vissa, N.K., 2022, "Thermodynamic changes in the atmosphere associated with pre-monsoon thunderstorms over eastern and north-eastern India". *Extreme natural events: sustainable solutions for developing countries*, 165-197. doi: https://10.1007/978-981-19-2511-5_7.

Varga, Á. J. and Breuer, H., 2020, "Sensitivity of simulated temperature, precipitation, and global radiation to different WRF configurations over the Carpathian Basin for regional climate applications", *Climate Dynamics*, **55**, 2849–2866. doi: https://10.1007/s00382-020-05416-x.

You, J., and Wang, S. 2021, "Higher probability of occurrence of hotter and shorter heat waves followed by heavy rainfall", *Geophysical Research Letters*, **48**, e2021GL094831. doi: https://10.1029/2021GL094831.